AD-A045 619 ROME AIR DEVELOPMENT CENTER GRIFFISS AFB N Y F/G 9/1
DESIGN OF PARABOLIC CYLINDER REFLECTOR SYSTEMS WITH LOW SIDELOB--ETC(U)
JUN 77 R L FANTE

UNCLASSIFIED RADC-TR-77-204 NL

1 OF 1
ADA045619

END
DATE FILMED
11-77
DDC

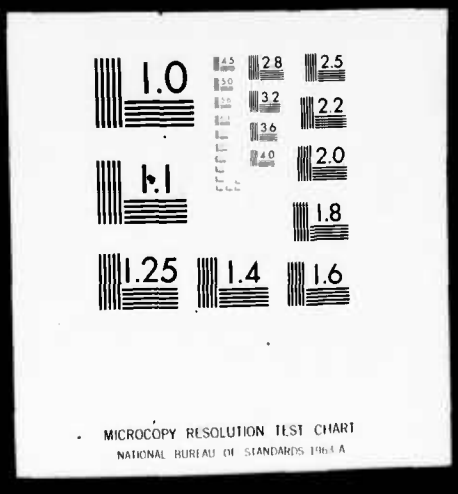

RADC-TR-77-204
IN-HOUSE REPORT
JUNE 1977

12

Design of Parabolic Cylinder Reflector Systems With Low Sidelobes

RONALD L. FANTE

ROME AIR DEVELOPMENT CENTER
AIR FORCE SYSTEMS COMMAND
GRIFFISS AIR FORCE BASE, NEW YORK 13441

This report has been reviewed by the RADC Information Office (OI) and is releasable to the National Technical Information Service (NTIS). At NTIS it will be releasable to the general public, including foreign nations.

This technical report has been reviewed and approved for publication.

APPROVED: Walter Rotman

WALTER ROTMAN
Chief, Microwave Detection Technques Branch
Electromagnetic Sciences Division

APPROVED: Allan C. Schell

ALLAN C. SCHELL
Acting Chief
Electromagnetic Sciences Division

FOR THE COMMANDER: John P. Huss

Plans Office

MISSION
of
Rome Air Development Center

RADC plans and conducts research, exploratory and advanced development programs in command, control, and communications (C^3) activities, and in the C^3 areas of information sciences and intelligence. The principal technical mission areas are communications, electromagnetic guidance and control, surveillance of ground and aerospace objects, intelligence data collection and handling, information system technology, ionospheric propagation, solid state sciences, microwave physics and electronic reliability, maintainability and compatibility.

Printed by
United States Air Force
Hanscom AFB, Mass. 01731

SECURITY CLASSIFICATION OF THIS PAGE (When Data Entered)

REPORT DOCUMENTATION PAGE	READ INSTRUCTIONS BEFORE COMPLETING FORM
1. REPORT NUMBER: RADC-TR-77-204	2. GOVT ACCESSION NO. / 3. RECIPIENT'S CATALOG NUMBER
4. TITLE (and Subtitle): DESIGN OF PARABOLIC CYLINDER REFLECTOR SYSTEMS WITH LOW SIDELOBES	5. TYPE OF REPORT & PERIOD COVERED: In House.
	6. PERFORMING ORG. REPORT NUMBER
7. AUTHOR(s): Ronald L. Fante	8. CONTRACT OR GRANT NUMBER(s)
9. PERFORMING ORGANIZATION NAME AND ADDRESS: Deputy for Electronic Technology (RADC/ETEP), Hanscom AFB, Massachusetts 01731	10. PROGRAM ELEMENT, PROJECT, TASK AREA & WORK UNIT NUMBERS
11. CONTROLLING OFFICE NAME AND ADDRESS: Deputy for Electronic Technology (RADC/ETEP), Hanscom AFB, Massachusetts 01731	12. REPORT DATE: June 1977 / 13. NUMBER OF PAGES: 40
14. MONITORING AGENCY NAME & ADDRESS(if different from Controlling Office)	15. SECURITY CLASS. (of this report): Unclassified / 15a. DECLASSIFICATION/DOWNGRADING SCHEDULE

16. DISTRIBUTION STATEMENT (of this Report)

Approved for public release; distribution unlimited.

17. DISTRIBUTION STATEMENT (of the abstract entered in Block 20, if different from Report)

18. SUPPLEMENTARY NOTES

309 050

19. KEY WORDS (Continue on reverse side if necessary and identify by block number)

Reflectors
Low sidelobe antennas
Radiation

20. ABSTRACT (Continue on reverse side if necessary and identify by block number)

We have determined and synthesized the feed distribution which must be used to illuminate an Offset Parabolic Cylinder in order to obtain a secondary radiation pattern with -50 dB sidelobes.

DD FORM 1 JAN 73 1473 EDITION OF 1 NOV 65 IS OBSOLETE

Unclassified

SECURITY CLASSIFICATION OF THIS PAGE (When Data Entered)

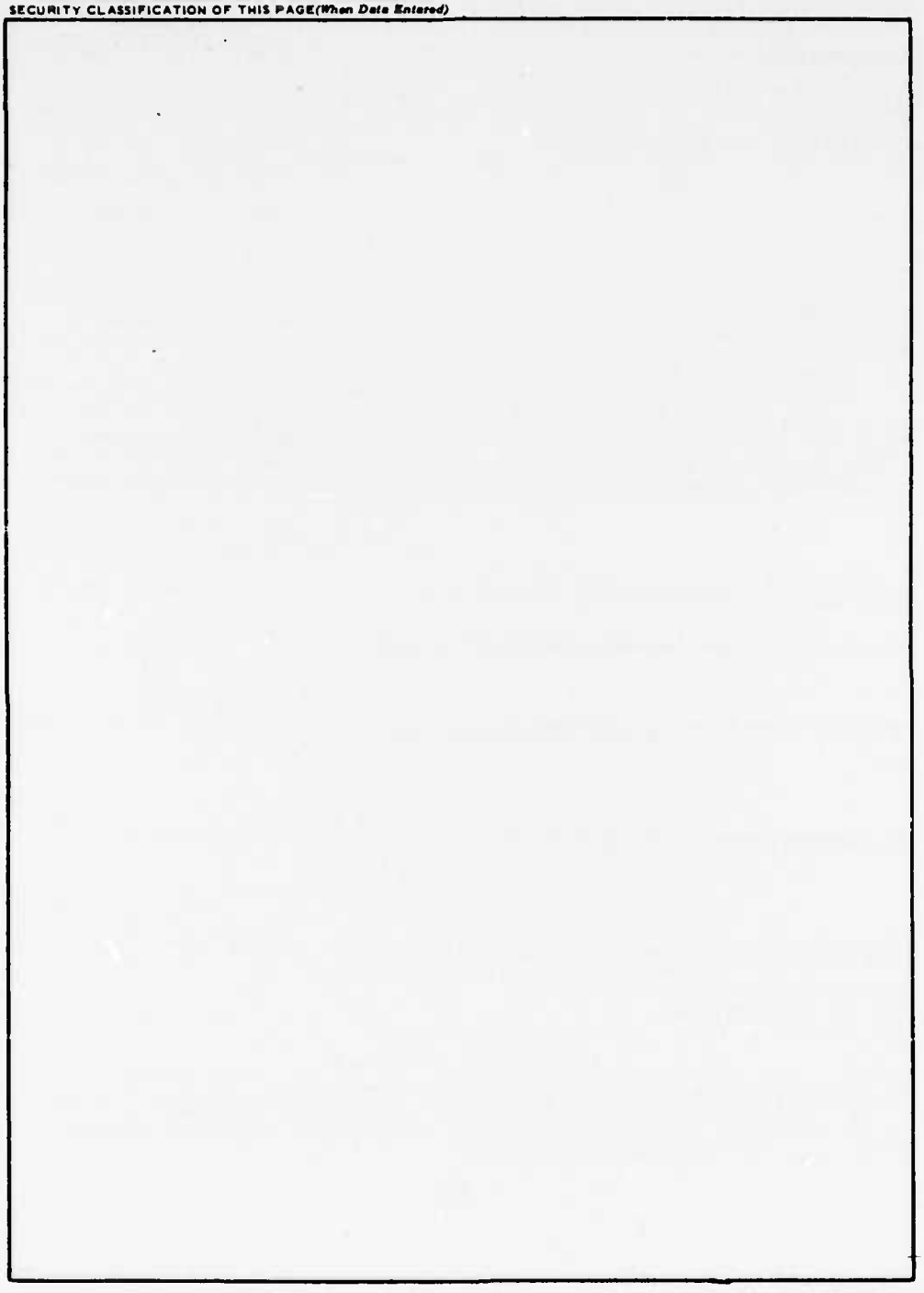

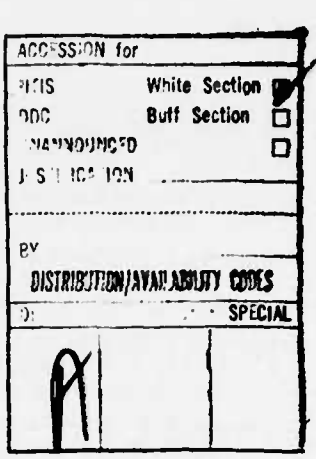

Contents

Illustrations

Illustrations

Tables

Design of Parabolic Cylinder Reflector Systems With Low Sidelobes

1. INTRODUCTION

In this report we will study the illumination required on an offset parabolic cylinder reflector in order to obtain a secondary radiation pattern with -50 dB sidelobes.

2. GENERAL REFLECTOR ANALYSIS

Let us consider an arbitrary cylindrical reflector with an arbitrarily located feed, as shown in Figure 1. The electric field incident on the reflector due to the line source feed can be written as

$$\underline{E}_i = \left[\hat{y}\, F_v(\psi) + \hat{\psi}\, F_H(\psi)\right] \frac{e^{-iks}}{\sqrt{s}} \tag{1}$$

where $\hat{y}$ is a unit vector normal to the paper $\hat{\psi} = \hat{x} \cos\psi + \hat{z} \sin\psi$, $\hat{x}$ and $\hat{z}$ are unit vectors along x and z respectively, s is the distance from the center of the feed to an arbitrary point P on the reflector, $F_v(\psi)$ is the field pattern of the vertically polarized signal and $F_H(\psi)$ is the field pattern of the horizontally polarized signal. The magnetic field incident on the reflector follows immediately from Eq. (1) and is

(Received for publication 17 June 1977)

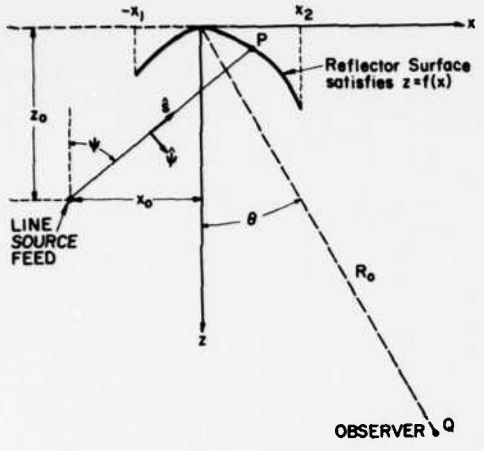

Figure 1. Reflector Geometry for Arbitrary Feed Location

$$\underline{H}_i = Y_o\,(\hat{s} \times \underline{E}_i) = Y_o\left[\hat{\psi}\,F_v(\psi) - \hat{y}\,F_H(\psi)\right]\frac{e^{-iks}}{\sqrt{s}} \tag{2}$$

where Y_o is the admittance of vacuum. The magnetic field scattered by the reflector when H_i is incident upon it can be calculated using the physical optics approximation.[1] This gives

$$\underline{H}_s = \left(\frac{ik}{2\pi R_o}\right)^{1/2} e^{-kR_o} \int_{-x_1}^{x_2} dx \left[\left(\hat{z} - \hat{x}\,\frac{\partial f}{\partial x}\right) \times \underline{H}_i\right] \times \left[\hat{x}\sin\theta + \hat{z}\cos\theta\right]$$
$$\cdot\ \exp\left[ik\,(x\sin\theta + z\cos\theta)\right] \tag{3}$$

where R_o is the distance from the center of the reflector to the field point Q and $z = f(x)$ is the equation satisfied by the reflector surface. Using Eq. (2) we have

$$\left(\hat{z} - \hat{x}\,\frac{\partial f}{\partial x}\right) \times \underline{H}_i = \frac{Y_o e^{-iks}}{\sqrt{s}}\left[\hat{x}\,F_H(\psi)\right.$$
$$\left. + \hat{y}\left(\cos\psi + \sin\psi\,\frac{\partial f}{\partial x}\right)F_V(\psi) + \hat{z}\,F_H(\psi)\,\frac{\partial f}{\partial x}\right]. \tag{4}$$

We now assume that the line source is located at the focal point of the reflector as shown in Figure 2. In this case it is easy to show that for a parabolic reflector, satisfying the equation $z = x^2/4F$, we can write s and $\partial f/\partial x$ in terms of ψ as

$$\frac{\partial f}{\partial x} = \tan\left(\frac{\psi}{2}\right) \tag{5a}$$

$$s = F\sec^2\left(\frac{\psi}{2}\right) \tag{5b}$$

1. Silver, S. (1965) Microwave Antenna Theory and Design, Dover, New York.

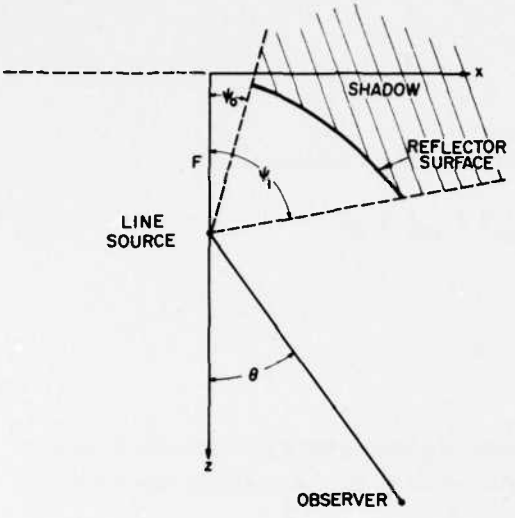

Figure 2. Offset Parabolic Reflector With Feed at the Focus

$$x = 2F \tan\left(\frac{\psi}{2}\right) \tag{5c}$$

$$z = F \tan^2\left(\frac{\psi}{2}\right) \tag{5d}$$

where F is the focal length of the reflector. If we now use Eqs. (5) and (4) in Eq. (3) and convert the integral from one over x to an integral over the variable ψ we get

$$\underline{H}_s = A \int_{\psi_0}^{\psi_1} d\psi \sec\left(\frac{\psi}{2}\right) \left[\hat{\theta}\, F_V(\psi) - \hat{y}\, F_H(\psi) (\cos\theta - \sin\theta \tan\frac{\psi}{2})\right]$$
$$\cdot \exp\left\{i\, 2k\, F \tan\left(\frac{\psi}{2}\right) \left[\sin\theta - \sin^2\left(\frac{\theta}{2}\right) \tan\left(\frac{\psi}{2}\right)\right]\right\} \tag{6}$$

where

$$A = \left(\frac{ik\, F}{2\pi\, R_o}\right)^{1/2} Y_o \exp\left[-ik\,(R_o + F)\right].$$

Also $\hat{\theta} = \hat{x} \cos\theta - \hat{z} \sin\theta$ = unit vector in θ-direction, and ψ_0, ψ_1 are the angular coordinates of the two end points of the reflector (shown in Figure 2).

It is now convenient to express the integral in Eq. (6) in terms of the dimensionless variable $u = \tan\psi/2$. We then have

$$H_s = 2A \int_{u_o}^{u_1} du (1+u^2)^{-1/2} \left[\hat{\theta}\, F_V(2\tan^{-1} u) - \hat{y}\, F_H(2\tan^{-1} u)(\cos\theta - u \sin\theta)\right]$$
$$\cdot \exp\left[i\, 2k\, Fu (\sin\theta - u \sin^2\frac{\theta}{2})\right] \tag{7}$$

where $u_1 = \tan(\psi_1/2)$ and $u_o = \tan(\psi_o/2)$.

3. ASYMPTOTIC EVALUATION OF Eq. (7)

For a vertically polarized field, Eq. (7) can be rewritten as

$$H_s = 2A \int_{u_0}^{u_1} du\, G(u) \exp\left[i\Omega (u - u^2 \sin^2\frac{\theta}{2} \sin^{-1}\theta)\right] \tag{8}$$

where $G(u) = (1 + u^2)^{-1/2} F_v(2 \tan^{-1} u)$,

$\Omega = 2kF \sin\theta$.

In the region $-(\pi + \psi_0) < \theta < (\pi - \psi_1)$ we can use the results in Appendix A to show that for large values of Ω the principal contribution to H_s comes from the edges of the reflector. In particular we find

$$H_s \simeq H_{eo} + H_{e1} \tag{9}$$

where

$$H_{eo} = -\left(\frac{2A}{i\Omega}\right) \frac{F_v(2\tan^{-1} u_o)(1 + u_o^2)^{1/2}}{(1 - 2u_o \sin^2\frac{\theta}{2} \sin^{-1}\theta)} \exp\left[i\Omega u_o(1 - u_o \sin^2\frac{\theta}{2} \sin^{-1}\theta)\right] \tag{10a}$$

$$H_{e1} = \left(\frac{2A}{i\Omega}\right) \frac{F_v(2\tan^{-1} u_1)(1 + u_1^2)^{1/2}}{(1 - 2u_1 \sin^2\frac{\theta}{2} \sin^{-1}\theta)} \exp\left[i\Omega u_1(1 - u_1 \sin^2\frac{\theta}{2} \sin^{-1}\theta)\right] \tag{10b}$$

Of course Eq. (9) is not valid for θ very near to zero because Ω is no longer large. In that regime, Eq. (8) must be evaluated numerically. Equation (9) is a good approximation everywhere else in the illuminated region, but fails at the shadow boundaries $\theta = -\pi - \psi_o$ and $\theta = \pi - \psi_1$. In the shadow region Eq. (9) is again a fair approximation as we shall see later. The use of physical optics integral in the shadow region has been investigated previously by M. Safak.[2] A corresponding analysis using GTD has been performed by C. Knop.[3]

---

2. Safak, M. (1976) Calculation of Radio Patterns of Reflector Antennas by High Frequency Asymptotic Techniques, Einhover University of Technology. Report 76-E-62.

3. Knop, C. (1976) On the front to back ratio of a parabolic dish antenna, IEEE Trans. AP-24:109-111.

It has become common to approximate the scattered fields by a pair of equivalent currents flowing along each edge of the reflector. Unfortunately, this approach is valid only over a small range of angles θ. In order to see this let us first recall that the magnetic field due to a line current I is given by

$$H = -\left(k/8\pi\rho\right)^{1/2} I \exp\left[-i\left(k\rho - \frac{\pi}{4}\right)\right] \tag{11}$$

where ρ is the distance from the source to the field point. Upon observing that the distance from the edge of $\psi = \psi_o$ to the field point is

$$\rho = R_o - 2F u_o\left(\sin\theta - u_o \sin^2\frac{\theta}{2}\right) - F u_o^2$$

and that the distance from the edge at $\psi = \psi_1$ to the field point is

$$\rho = R_o - 2F u_1\left(\sin\theta - u_1 \sin^2\frac{\theta}{2}\right) - F u_1^2$$

we readily see by equating Eq. (11) to Eqs. (10a) and (10b) that the equivalent currents on the edges at $\psi = \psi_o$ and $\psi = \psi_1$ are, respectively

$$I_o = \frac{2Y_o F_v\left(2\tan^{-1} u_o\right)\left(1 + u_o^2\right)^{-1/2}}{ikF^{1/2}\left(\sin\theta - 2u_o \sin^2\frac{\theta}{2}\right)} e^{-ikF(u_o^2 + 1)} \tag{12a}$$

$$I_1 = \frac{2Y_o F_v\left(2\tan^{-1} u_1\right)\left(1 + u_1^2\right)^{-1/2}}{ikF^{1/2}\left(\sin\theta - 2u_1 \sin^2\frac{\theta}{2}\right)} e^{-ikF(u_1^2 + 1)} \tag{12b}$$

We note that the equivalent currents depend on θ; this is impossible because the equivalent current should not depend on the direction of observation. We must therefore conclude that the equivalent current method is valid only over a narrow range of angles θ.

4. USE OF Eq. (9) IN THE SHADOW REGION

The physical-optics approximation in Eq. (8) is known to be a good approximation in the illuminated region, but we would not expect it to be valid in the shadow region ($\theta > \pi - \psi_1$). An asymptotic evaluation of Eq. (8) for large values of Ω shows that Eq. (8) can be approximated by the edge contributions in Eq. (9) plus a contribution due to a stationary point in the integral which occurs at $u = 0.5 \sin\theta/\sin^2(\theta/2)$. That is, in the shadow region (but not too near to the shadow boundary) we find using Appendix A that

$$H_s = H_{eo} + H_{el} + H_{st} \tag{13}$$

where

$$H_{st} = 2A\left(\frac{\pi}{2kF}\right)^{1/2} F_v\left[2\tan^{-1}\left(\frac{\sin\theta}{1-\cos\theta}\right)\right] \exp\left[i\frac{\Omega}{2}\left(\frac{\sin\theta}{1-\cos\theta}\right) - i\frac{\pi}{4}\right] \tag{14}$$

and H_{eo} and H_{el} are given in Eqs. (10a) and (10b). A study of Eq. (13) indicates that the contribution from the stationary point* does not correspond to any ray which could be physically diffracted into the shadow region. Therefore, we would expect that this term should be ignored and the magnetic field in the shadow approximated is

$$H_s = H_{eo} + H_{el}\,. \tag{15}$$

That is, the total shadow field is the sum of the fields diffracted by the edges as calculated by the physical optics approximation. We now desire to compare these physical optics diffraction coefficients with those calculated using the geometrical theory of diffraction. Let us therefore consider the field at $\theta = \pi$ which is diffracted by the edge at $\psi = \psi_1$. From classical diffraction theory we know that the diffraction coefficient D_p is related to the edge current I via

$$I = -(8\pi/k)^{1/2}\, e^{-i\frac{\pi}{4}}\, Y_o\, D\, E_i \tag{16}$$

where E_i is the electric field incident on the edge. For a vertically polarized field we have from Eq. (1) that

$$E_i = \frac{F_v\left(2\tan^{-1} u_1\right)\exp\left[-ikF\left(1+u_1^2\right)\right]}{F^{1/2}\left(1+u_1^2\right)^{1/2}}\,. \tag{17}$$

Therefore from Eqs. (12b) and (14) we have that

$$I_1 = \frac{-Y_o\, E_i\, e^{-i(\pi/2)}}{kF^{1/2}\, u_1}\,. \tag{18}$$

Upon equating Eqs. (16) and (18) we find that the physical optics diffraction coefficient is

*The contribution from the stationary point does not arise when analyzing the front to back ratio of the paraboloid reflector because the integrand vanishes at the stationary point in this case.

$$D_p = \frac{e^{-i\frac{\pi}{4}}}{2(2\pi k)^{1/2}\, u_1} = \frac{e^{-i\frac{\pi}{4}} \cos\left(\frac{\psi_1}{2}\right)}{2(2\pi k)^{1/2} \sin\left(\frac{\psi_1}{2}\right)}. \tag{19a}$$

From the geometrical theory of diffraction we find[4]

$$D_g = \frac{e^{-i\frac{\pi}{4}} \left[1 - \sin\left(\frac{\psi_1}{2}\right)\right]}{2(2\pi k)^{1/2} \sin\left(\frac{\psi_1}{2}\right)}. \tag{19b}$$

The ratio of D_p/D_g for some values of ψ_1 of interest is given in Table 1. From Table 1 we see that the physical optics approximation leads to diffraction coefficients which are in the same ballpark as those calculated by the geometrical theory of diffraction. Consequently, in most cases of interest we shall be able to use Eq. (9) to get a "ballpark" estimate of the field, even in the shadow.

Table 1. The Ratio of D_p/D_g for Some Values of ψ_1

ψ_1 (degrees)	$\frac{D_p}{D_g}$
30	1.3
45	1.5
60	1.73
75	2.04

The difference between D_p and D_g is an indication that the physical optics current $\underline{J}_p = 2(\hat{n} \times \underline{H}_i)$ is not exact near the edges of the reflector, and that a correction term $\underline{J}_c$ is required so that $\underline{J} = \underline{J}_p + \underline{J}_c$, as suggested by Ufimtsev.[5]

5. SMALL θ APPROXIMATION

The approximate result in Eq. (9) is valid only for $2kF \sin\theta >> 1$ and consequently cannot be used for small values of θ. For values of θ sufficiently small

4. James G., and Kerdemelidas, V. (1973) Reflector antenna radiation pattern analysis by equivalent edge currents, IEEE Trans. AP-21:19-24, (we have used Eq. (8) with $\Phi_o = \pi - \psi/2$, $\Phi = 3\pi + \psi/2$).

5. Ufimtsev, B. (1975) Comparison of three HF defraction techniques, Proc. IEEE 63:1734-1737.

that $\theta << (2/kF)^{1/2}$ we can approximate $\exp[-i2kF u^2 \sin^2(\theta/2)]$ by unity and $\sin\theta$ by θ. In this case Eq. (7) becomes

$$H_s \simeq 2A \int_{u_0}^{u_1} \frac{du}{(1+u^2)^{1/2}} \left[\hat{\theta} F_v (\tan^{-1} u) - \hat{y} F_H (2 \tan^{-1} u)\right] e^{i2kFu\theta} \qquad (20)$$

By using Eq. (20) one could readily obtain the feed distribution necessary to obtain a prescribed radiation field $H_p(\theta)$ for small θ. For a vertically polarized field ($F_H = 0$) we find,

$$F_v(\psi) = B \sec\left(\frac{\psi}{2}\right) \int_{-\infty}^{\infty} d\theta\, H_p(\theta) \exp\left[-i2kF\theta \tan\left(\frac{\psi}{2}\right)\right] \qquad (21)$$

where B is a constant. Equation (21) was obtained from Eq. (20) by multiplying Eq. (20) by $\exp(-i2kFu'\theta)$ and integrating on θ.

By using Eqs. (9) and (20) we can get an estimate of the ratio of the magnitude of the near-in sidelobes of the reflector to the mean beam magnitude. If we assume that the feed horn is pointed at the center of the reflector as shown in Figure 3 and has a symmetric pattern with the peak at P then

$$\left|\frac{H_s(\theta)}{H_s(0)}\right|^2 \simeq 2\left(\frac{2}{kF}\right)^2 \left|\frac{F_v(\psi_e)}{F_v(0)}\right|^2 \left(\frac{1}{\theta\psi_B}\right)^2 \qquad (22)$$

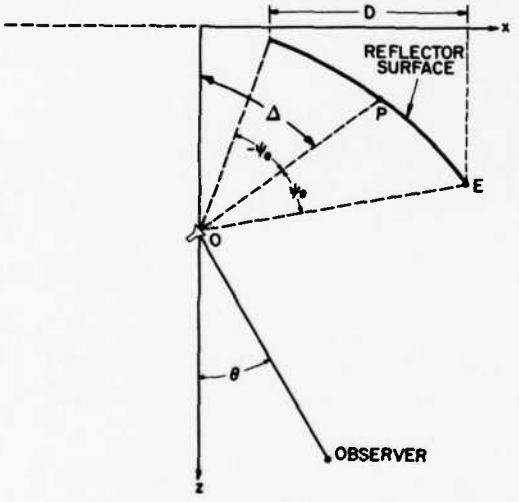

Figure 3. Geometry Assumed for Eq. (22)

where $F_v(0)$ corresponds to the field in the direction OE in Figure 3 and ψ_B is the total angle subtended by the reflector. For example the sidelobe $\theta = 5.7°$ from a reflector with $\psi_B = \pi/2$, an edge taper of -36 dB, and kF = 188.5 is predicted by Eq. (22) to be -56.6 dB. An exact calculation from Eq. (7) gives -55.7 dB.

6. NUMERICAL COMPUTATIONS

In order to design a parabolic cylinder reflector system with very low sidelobes everywhere, it is clear from Eq. (22) that one necessary condition is that the edge illumination be quite small compared with the illumination at the center of the reflector. However, this is not enough because the tolerances on the manufacture of the reflector surface must also be held very close, and in addition, we must require that there be very little spillover of the radiation field of the feed system beyond the edges of the reflector. For example, if we require that all of the reflector sidelobes be more than 50 dB below the main beam, and the gain of the reflector is 14 dB, then the sidelobes of the feed antenna must be more than 36 dB down from the peak of the feed antenna pattern. If the feed-antenna sidelobes were no problem we could easily obtain very small values of $F_v(\psi_e)/F_v(0)$ with a conventional (with phase correction) horn with TE_{10} mode across its aperture. However, as we clearly see from Figure 4 this leads to sidelobes which are too large. One way to get low feed antenna sidelobes is to allow higher order modes in the feed distribution. The rationale for this is presented in Appendix B. When the horn aperture distribution consists of a TE_{10} mode plus 0.1666 of a TE_{30} mode it is evident from Figure 4 that the feed-antenna pattern is satisfactory. We have not extended our plots beyond $\psi = \pm 90°$, because we have used the result of Chu[6]

$$F_v(\psi) = C_1 \cos\left(\frac{\pi b}{\lambda}\sin\psi\right)\left[\frac{(T_1 + \cos\psi)}{\left(\frac{2b}{\lambda}\sin\psi\right)^2 - 1} - \frac{3\alpha(T_3 + \cos\psi)}{\left(\frac{2b}{\lambda}\sin\psi\right)^2 - 9}\right] \tag{23}$$

for the radiation pattern of a rectangular waveguide with a TE_{10} mode plus a fraction α of TE_{30} mode, and this result is of doubtful validity for $|\psi| > 90°$. In Eq. (23) C_1 is a constant and b is the length of the feed aperture (the electric field across the feed aperture is assumed to be $\cos\frac{\pi y}{b} + \cos(\frac{3y\pi}{b})$ and $T_n = [1 - (\frac{n\lambda}{2b})^2]^{1/2}$.

A computer program has been written which utilizes Eq. (7) to calculate the radiation pattern of the reflector. When F_v is given by Eq. (23) with $b = 2.7\lambda$ and $\alpha = 0.1666$ it is found that for a reflector with $\psi_o = 0°$, $\psi_1 = 90°$, $\Delta = 45°$, and kF = 188.5 the radiation pattern is as shown* in Figure 5. We observe that all sidelobes are less than 50 dB below the main beam.

6. Chu, L. (1940) Calculation of the radiation properties of hollow pipes and horns, J. Appl. Phys. 11:603-610.

*In obtaining Figures 6 to 8 we have ignored the scattering by the feed element. Feed scatter (or aperture blockage) gives rise to sidelobe levels which are about 61 dB below the main beam level.

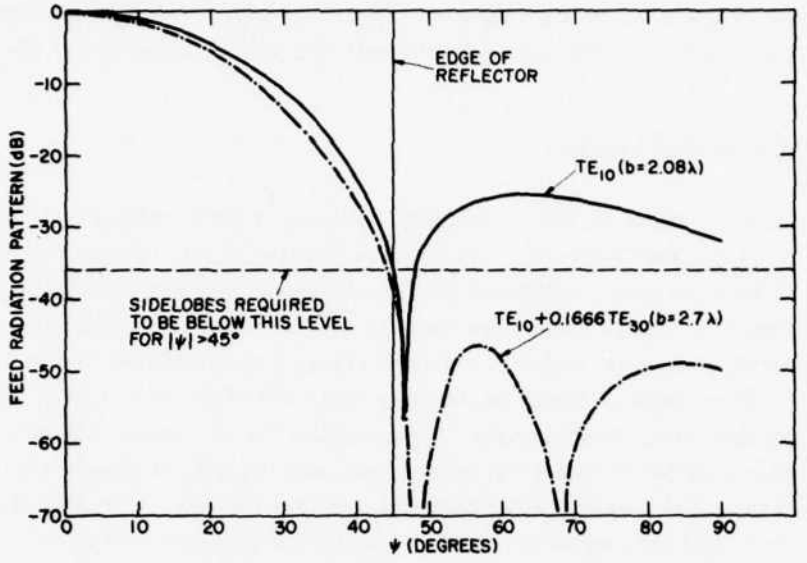

Figure 4. Radiation Patterns of Planar Feed Apertures for Different Mode Distributions

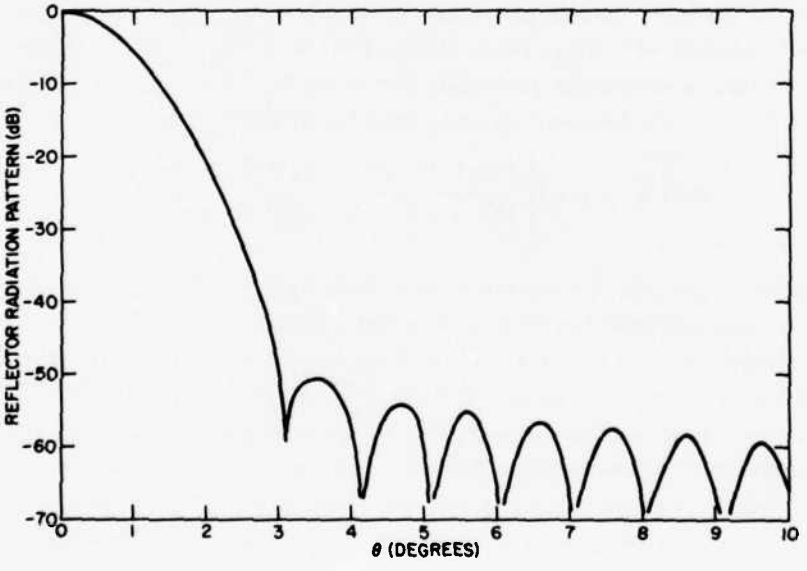

Figure 5. Radiation Pattern of a Reflector With $\psi_o = 0$, $\psi_1 = 90°$, $\Delta = 45°$, $2\pi F/\lambda = 188.5$ Illuminated by a Feed Aperture With $b = 2.7\lambda$ and Having a $TE_{10} + 0.1666\ TE_{30}$ Distribution

We would now like to put all our previous ideas together to design a parabolic cylinder antenna with a 2° (3 dB) beamwidth and -50 dB sidelobes which can operate from 3.1 to 3.6 GHz. We choose a reflector which satisfies $z = x^2/4F$ and pick $\psi_o = 5°$, $\psi_1 = 80°$, $\Delta = 42.5°$ and $F = 8.802$ feet. This leads to a cylindrical reflector with a diameter (see Figure 3) of 14 feet. This reflector has a gain of 14 dB so that in order to get sidelobes smaller than -50 dB we require a feed antenna such that: (1) the edge illumination on the reflector is -36 dB below the illumination at the center and (2) the spillover of the feed pattern beyond the edges of the reflector must be smaller than -36 dB (relative field smaller than 0.016). This can be achieved by a planar aperture of width b = 10.895 in. with a $TE_{10} + \alpha\ TE_{30}$ distribution. Typical feed (E-field) radiation patterns $F_v(\psi)$ are shown in Figure 6 for different values of α for a frequency (3.35 GHz) at the middle of the required operating band. By making similar plots for 3.1 GHz and 3.6 GHz, we have found that $\alpha = 0.14$ is a good compromise value which leads to edge illuminations below -36 dB and spillover below -36 dB over the entire band of operation (3.1 to 3.6 GHz). If we choose $\alpha = 0.14$ and assume that the feed aperture distribution remains $TE_{10} + 0.14\ TE_{30}$ over the entire frequency band (3.1 to 3.6 GHz) then we obtain the radiation patterns shown in Figures 7 to 9 for f = 3.1 GHz, 3.35 GHz and 3.6 GHz, respectively. Observe that the 3 dB beamwidth is approximately 1.8° and that the sidelobes are generally well below -50 dB over the entire band.

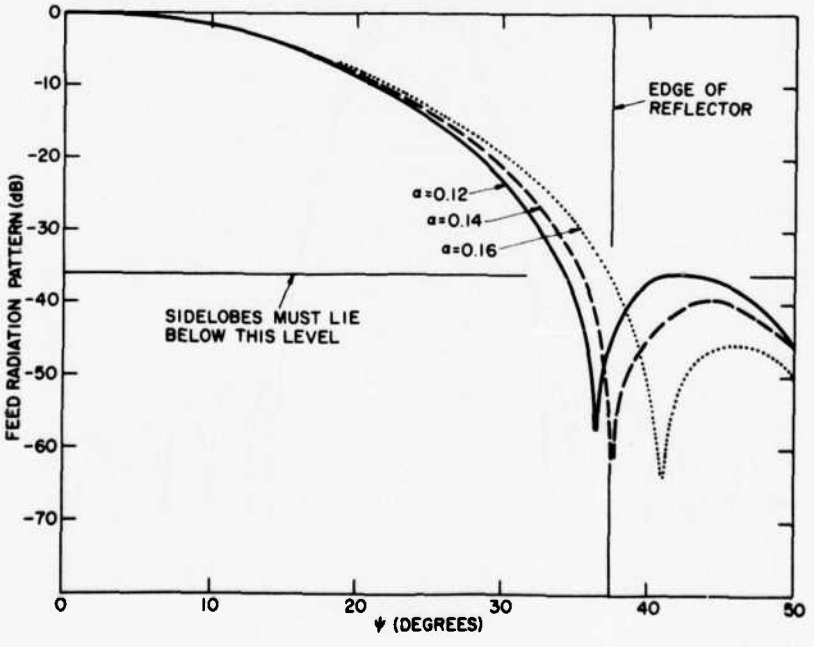

Figure 6. Effect of Varying α on the Radiation Pattern of a Planar Aperture With b = 3.09λ = 10.895 in. at a frequency of 3.35 GHz

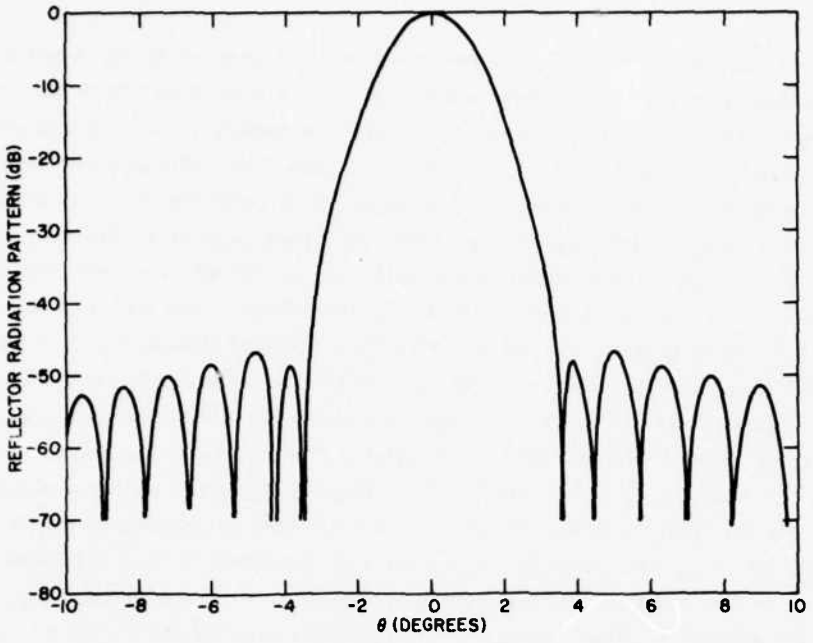

Figure 7. Radiation Pattern at 3.1 GHz of a Parabolic Cylinder With $\psi_o = 5°$, $\psi_1 = 80°$, $\Delta = 42.5°$, F = 8.8002 ft Illuminated by a Feed Aperture With b = 10.895 in. and $\alpha = 0.14$

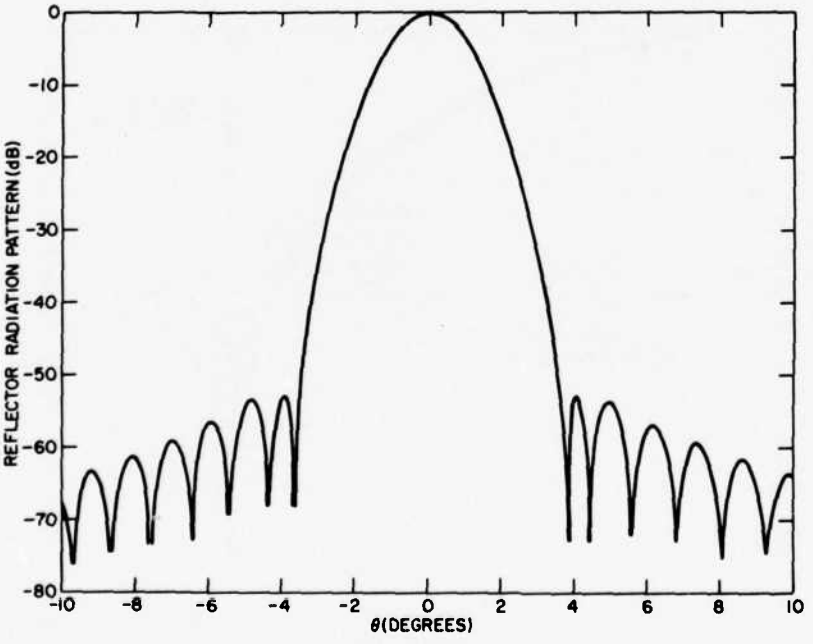

Figure 8. Radiation Pattern at 3.35 GHz of a Parabolic Cylinder With $\psi_o = 5°$, $\psi_1 = 80°$, $\Delta = 42.5°$, F = 8.8002 ft Illuminated by a Feed Aperture With b = 10.895 in. and $\alpha = 0.14$

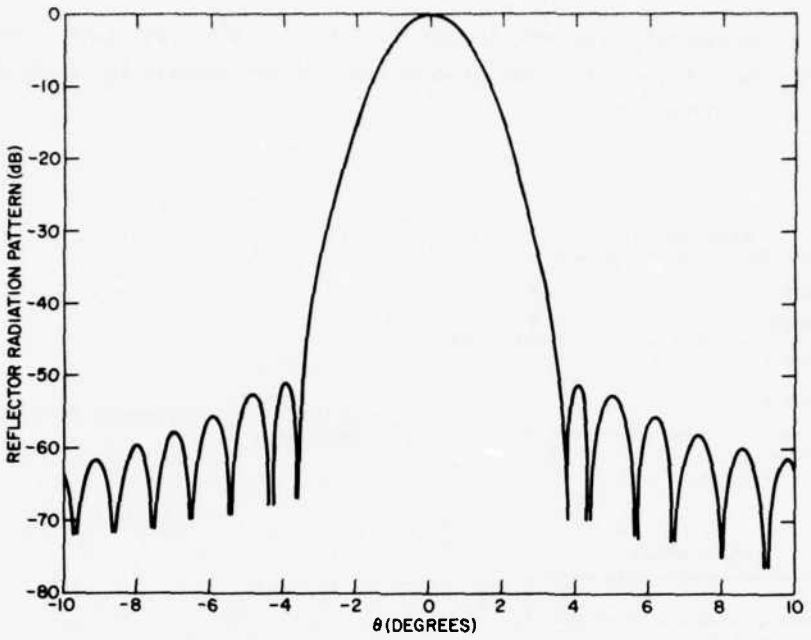

Figure 9. Radiation Pattern at 3.6 GHz of a Parabolic Cylinder With $\psi_o = 5°$, $\psi_1 = 80°$, $\Delta = 42.5°$, F = 8.8002 ft Illuminated by a Feed Aperture With b = 10.895 in. and $\alpha = 0.14$

In the next section of this report we will discuss a method for achieving a feed distribution consisting of $TE_{10} + 0.14\ TE_{30}$ modes over a planar aperture which is approximately 3 wavelengths wide.

7. FEED DESIGN

We now discuss a feed design which can give the low-spillover we require. In particular we desire that the feed aperture be 3.09 wavelengths wide at 3.35 GHz with an aperture distribution of $TE_{10} + 0.14\ TE_{30}$ modes. In addition we shall require that the feed be compact (less than 1-ft long) and not contain any lenses. These requirements force us to exclude horns because they would have to be too long in order to have small quadratic phase errors across the aperture. The design we actually chose was suggested by W. Rotman and is shown in Figure 10. Because $b = 3.09\lambda$ it is clear that all modes up to the TE_{60} can propagate, whereas we want only the TE_{10} plus TE_{30}. If the feed probes are asymmetrically located about the center of the guide then the TE_{20}, TE_{40} and TE_{60} will not be excited. Moreover if the probes are located at the zeros of the TE_{50}, as shown, then this

mode will not be excited. Therefore, only the TE_{10} and TE_{30} will exist. We will now calculate the probe currents required to produce the required fractions of TE_{10} and TE_{30} modes.

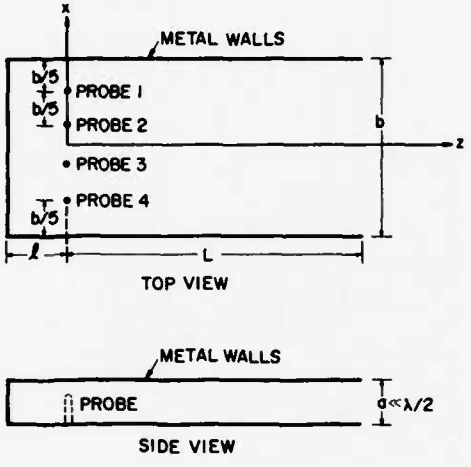

Figure 10. Geometry of the Feed Antenna

In the region $z < 0$ in Figure 10 we can write the electric field as

$$\underline{E} = \hat{y} \sum_{n=1}^{\infty} C_n \sin\left(\frac{n\pi x}{b}\right) \sinh \Gamma_n (z + \ell) \tag{24}$$

whereas for $z > 0$ we have

$$\underline{E} = \hat{y} \sum_{n=1}^{\infty} \left(D_n e^{-\Gamma_n z} + R_n e^{\Gamma_n z} \right) \sin\left(\frac{n\pi x}{b}\right) \tag{25}$$

where $\hat{y}$ is a unit vector, $\Gamma_n^2 = (n\pi/b)^2 - (2\pi/\lambda)^2$, λ = wavelength, and C_n, D_n, and R_n are unknown coefficients. Because the aperture is more than 3 wavelengths wide we expect that the reflection coefficient R_n will be small for both the TE_{10} and TE_{30} modes. If we ignore R_n and require that the electric field be continuous across the $z = 0$ plane we get

$$C_n \sin \Gamma_n \ell = D_n . \tag{26}$$

If we assume that the probes are infinitesimally thin we can write their total current density as

$$\underline{J} = \hat{y} \sum_{p=1}^{4} \beta_p \, \delta(z) \, \delta(x - x_p) \tag{27}$$

where β_p is to be calculated and $x_p = pb/5$. Then from Maxwell's wave equation we have

$$\frac{\partial^2 E}{\partial x^2} + \frac{\partial^2 E}{\partial z^2} + k^2 E = i\omega\mu_o \, \delta(z) \sum_{p=1}^{4} \beta_p \, \delta(x - x_p) . \tag{28}$$

If we multiply Eq. (28) by $\sin(n\pi x/b)$ and integrate we get

$$\frac{d^2 e_n}{dz^2} + \left(k^2 - \frac{n^2\pi^2}{b^2}\right) e_n = i\omega\mu_o \, \delta(z) \sum_{p=1}^{4} \beta_p \sin\left(\frac{n\pi x_p}{b}\right) \tag{29}$$

where

$$e_n = \int_0^b dx \sin\left(\frac{n\pi x}{b}\right) E(x, z) .$$

Upon integrating Eq. (29) from $z = 0^-$ to $z = 0^+$ we find

$$\left(\frac{de_n}{dz}\right)_{0^-}^{0^+} = i\omega\mu_o \sum_{p=1}^{4} \beta_p \sin\left(\frac{n\pi x_p}{b}\right) . \tag{30}$$

If we use Eqs. (24) and (25) in Eq. (30) we get

$$\Gamma_n D_n + C_n \Gamma_n \cosh \Gamma_n \ell = -i\omega\mu_o \sum_{p=1}^{4} \beta_p \sin\left(\frac{n\pi x_p}{b}\right) . \tag{31}$$

Finally upon combining Eqs. (26) and (31) we get

$$D_n = \frac{-i\omega\mu_o}{\Gamma_n (1 + \coth \Gamma_n \ell)} \sum_{p=1}^{4} \beta_p \sin\left(\frac{n\pi x_p}{b}\right) . \tag{32}$$

When there is perfect symmetry and $x_p = \frac{pb}{5}$ we find that only D_1 (TE_{10} mode) and D_3 (TE_{30} mode) are nonzero. From Eq. (32) we can then solve for $\beta_1 = \beta_4$ and $\beta_2 = \beta_3$ in terms of D_1 and D_3. If we require that the aperture distribution consist of a TE_{10} mode plus α of a TE_{30} mode then

$$D_3 = \alpha \exp\left[(\Gamma_3 - \Gamma_1) L\right] D_1 . \tag{33}$$

We then find from Eqs. (32) and (33) that

$$\beta_1 = 0.47022 + 0.76084 \left(\frac{\Gamma_3}{\Gamma_1}\right)\left(\frac{1 + \coth \Gamma_3 \ell}{1 + \coth \Gamma_1 \ell}\right) \alpha \exp\left[(\Gamma_3 - \Gamma_1) L\right] \tag{34}$$

$$\beta_2 = 0.76084 - 0.47022\left(\frac{\Gamma_3}{\Gamma_1}\right)\left(\frac{1 + \coth \Gamma_3 \ell}{1 + \coth \Gamma_1 \ell}\right) \alpha \exp\left[(\Gamma_3 - \Gamma_1) L\right]. \tag{35}$$

For a system operating at 3.35 GHz with L = 8.12 in., ℓ = 0.88 in., and b = 10.90 in. we find

$$\beta_1 = \beta_4 = 0.588909 \exp(-i\, 16.07193°),$$

$$\beta_2 = \beta_3 = 1.$$

Unfortunately, it is generally impossible to locate each probe at precisely the correct location and to achieve precisely the desired amplitude and phase for its current. We have used Eq. (32) to study the effect of these errors. For example, suppose the required value of β on the p^{th} probe is $\beta_p{}^\circ = |\beta_p{}^\circ| \exp(i\, \phi_p{}^\circ)$. Because of phase and amplitude errors we get instead

$$\beta_p = r_p\, |\beta_p{}^\circ| \exp[i\, \phi_p{}^\circ + i\, \delta\, \phi_p].$$

Also, suppose the error in probe position is ϵ_p. Then including errors we have

$$\tilde{D}_n = \frac{-i\omega\mu_o}{\Gamma_n (1 + \coth \Gamma_n \ell)} \sum_{p=1}^{4} r_p\, |\beta_p{}^\circ|\, e^{i\phi_p{}^\circ + i\delta\phi_p} \sin\left(\frac{n\pi p}{5} + \frac{n\pi\epsilon_p}{b}\right). \tag{36}$$

This leads to an aperture distribution

$$E_{AP} = \sum_{n=1}^{\infty} \tilde{D}_n \exp(-\Gamma_n L) \sin\left(\frac{n\pi x}{b}\right) \tag{37}$$

and a corresponding feed radiation field

$$E(\psi) = \sum_{n=1}^{\infty} \tilde{D}_n \left(\frac{n\pi}{b}\right) \exp\left(-\Gamma_n L\right)\left(\frac{B_n}{k} + \cos\psi\right) \frac{\sin\left(\frac{\pi b}{\lambda}\sin\psi + \frac{n\pi}{2}\right)}{\left(\frac{\pi b}{\lambda}\sin\psi\right)^2 - \left(\frac{n\pi}{2}\right)^2} 2 \tag{38}$$

where

$$\frac{B_n}{k} = \left[1 - (n\lambda/2b)^2\right]^{1/2}.$$

We have studied the effect of all the errors on the feed radiation pattern. We have found that the tolerances required to meet the low spillovers specified are

$$\begin{aligned} \frac{\epsilon_p}{b} &= \pm\ 0.0015, \\ \delta\phi_p &= 2.5°, \\ |r_p| &= 1 \pm 0.035. \end{aligned} \tag{39}$$

References

1. Silver, S. (1965) Microwave Antenna Theory and Design, Dover, New York.
2. Safak, M. (1976) Calculation of Radio Patterns of Reflector Antennas by High Frequency Asymptotic Techniques, Einhover University of Technology, Report 76-E-62.
3. Knop, C. (1976) On the front to back ratio of a parabolic dish antenna (IEEE Trans. AP-24:109-111.
4. James, G., and Kerdemelidas, V. (1973) Reflector antenna radiation pattern analysis by equivalent edge currents, IEEE Trans. AP-21:19-24, (we have used Eq. (8) with $\Phi_o = (\pi-\psi)/2$, $\Phi = (3\pi+\psi)/2$).
5. Ufimtsev, B. (1975) Comparison of three HF defraction techniques, Proc. IEEE 63:1734-1737.
6. Chu, L. (1940) Calculation of the radiation properties of hollow pipes and horns, J. Appl. Phys. 11:603-610.
7. Felsen, L., and Marcuvitz, N. (1973) Radiation and Scattering of Waves, Prentice Hall, New York.
8. Slepian, D., and Pollak, H. (1961) Prolate spheroidal wave functions, Fourier Analysis and Uncertainty I, Bell System Tech. J. 40:43-74.

Appendix A

Asymptotic Formulae

For large Ω the integral

$$N(\Omega) = \int_{u_o}^{u_1} f(u)\, e^{i\Omega\psi(u)}\, du \tag{A1}$$

can be evaluated as[7]

$$N(\Omega) = N_s(\Omega)\, H[(u_s-u_o)(u_1-u_s)] + N_e(\Omega) + o(\Omega^{-3/2}) \tag{A2}$$

where u_s is the solution of $d\psi/du = 0$, H(t) is the unit step function, and

$$N_s(\Omega) = \left[\frac{2\pi}{|\Omega\psi_{uu}(u_s)|}\right]^{1/2} f(u_s)\, \exp\left[i(\Omega\psi(u_s) \pm \tfrac{\pi}{4})\right] \text{ for } \Omega\,\psi_{uu} \gtrless 0\,, \tag{A3}$$

$$N_e(\Omega) = \frac{f(u_1)\, e^{i\Omega\psi(u_1)}}{i\Omega\psi_u(u_1)} - \frac{f(u_o)\, e^{i\Omega\psi(u_o)}}{i\Omega\,\psi_u(u_o)}\,. \tag{A4}$$

The upper sign in Eq. (A3) is for $\Omega\psi_{uu} > 0$ and the lower is for $\Omega\psi_{uu} < 0$. $\psi_u = d\psi/du$, $\psi_{uu} = d^2\psi/du^2$. Also Eq. (A2) is written for the case when there is one stationary

7. Felsen, L., and Marcuvitz, N. (1973) Radiation and Scattering of Waves, Prentice Hall, New York.

point u_s; if there are more than one we simply sum over the different stationary points.

The result in Eq. (A2) is valid so long as the stationary point u_s does not approach either end point u_s or u_1. When $u_s \to u_o$ or $u_s \to u_1$ a more careful treatment is necessary. For the case when u is near u_o we get

$$N(\Omega) = N_e(\Omega) + N_s(\Omega)\ W(S_o\, e^{\mp i\frac{\pi}{4}}) \text{ for } \Omega\psi_{uu} \gtrless 0 \tag{A5}$$

where

$$S_o = \pm \left[\, |\Omega[\psi(u_s) - \psi(u_o)]| \,\right]^{1/2} \text{ for } (u_o - u_s) \gtrless 0\,,$$

$$W\left(S_o e^{\mp i\frac{\pi}{4}}\right) = Q\left(S_o\, e^{\mp i\frac{\pi}{4}}\right) - \frac{e^{+i\left(S_o^{\,2} + \frac{\pi}{4}\right)}}{2(\pi)^{1/2}\, S_o} \tag{A6}$$

$$Q\left(S_o e^{\mp i\frac{\pi}{4}}\right) = (\pi)^{-1/2} \exp\left(\mp i\tfrac{\pi}{4}\right) \int_{S_o}^{\infty} dt \exp\left(\pm i\, t^2\right).$$

We note that

$$Q(0) = \frac{1}{2}$$

$$Q\left(S_o e^{\mp i\frac{\pi}{4}}\right) = H(-S_o) + \frac{e^{+i\left(S_o^{\,2} + \frac{\pi}{4}\right)}}{2S_o(\pi)^{1/2}} \text{ for } |S_o| \to \infty\,.$$

On the shadow boundary ($u_s = u_o$) we then find from Eq. (A6) that (for $u_s > u_o$)

$$W\left(S_o\ e^{\mp i\frac{\pi}{4}}\right) = \frac{1}{2} + \frac{e^{+i\frac{\pi}{4}}}{2(\pi)^{1/2}\ |\Omega\,[\psi(u_s) - \psi(u_o)]|^{1/2}}\,. \tag{A7}$$

If we recall that $\psi(u)$ can be expanded in a Taylor series about u_s as

$$\psi(u) = \psi(u_s) + \tfrac{1}{2}\,\psi_{uu}\,(u_s)\,(u - u_s)^2 + \ldots \tag{A8}$$

we can rewrite Eq. (A7) as

$$W\left(S_o e^{\mp i\frac{\pi}{4}}\right) = \frac{1}{2} + \frac{e^{+i\frac{\pi}{4}}}{2(\pi)^{1/2}\ \left|\frac{\Omega}{2}\,\psi_{uu}(u_s)\,(u_o - u_s)^2\right|^{1/2}}\,. \tag{A9}$$

If we then use Eqs. (A9), (A3), and (A4) in (A5) we finally obtain for the shadow boundary

$$N_b(\Omega) = \frac{f(u_1)\, e^{i\Omega\psi(u_1)}}{i\Omega\psi_u(u_1)} + \frac{1}{2}\left(\frac{2\pi}{|\Omega\psi_{uu}(u_s)|}\right)^{1/2} f(u_s)\, \exp\left\{i\left[\Omega\psi(u_s) \pm \frac{\pi}{4}\right]\right\}$$

$$\text{for } \Omega\psi_{uu} \gtrless 0 \,. \tag{A10}$$

Therefore, there is no singularity on the shadow boundary $u_s = u_o$. A similar procedure follows for the shadow boundary $u_s = u_1$.

Appendix B

Optimum Synthesis

We will now show how one can approximately synthesize a low-sidelobe radiation pattern. We shall assume $F_H = 0$ and then set

$$t = au + b$$

where

$$a = \frac{2}{u_1 - u_o}$$

$$b_o = -\left(\frac{u_1 + u_o}{u_1 - u_o}\right).$$

Then we can rewrite Eq. (20) as

$$H_s(\sin\theta) = e^{-i\left(\frac{2kFb_o}{a}\right)\sin\theta} \int_{-1}^{1} dt\, G(t)\, e^{i\left(\frac{2kF}{a}\right)\sin\theta} \tag{B1}$$

where

$$G(t) = \frac{2AF_v\left[2\tan^{-1}\left(\frac{t-b_o}{a}\right)\right]}{\left[a^2 + (t-b_o)^2\right]^{1/2}} \tag{B2}$$

We note that Eq. (B1) is the standard form for the radiation pattern of a line source. Of course, it is not accurate for all values of θ because in writing Eqs. (20) and (B1) we have neglected the quadratic phase term $\exp[-i\,2k\,Fu^2\,\sin^2(\theta/2)]$. However, our synthesis method will be to temporarily neglect this term, obtain a distribution which gives low sidelobes with this term neglected, and then use this distribution in the exact integral in Eq. (7) to see what actual field is obtained when the term $\exp[-i\,2k\,Fu^2\,\sin^2(\theta/2)]$ is included.

Our procedure for obtaining low sidelobe will be to maximize the energy in the main lobe while keeping the total radiated energy fixed. The energy in the main lobe can be written as

$$\int_{-u_o}^{u_o} |H_s(u)|^2\,du = \sin\theta_o \int_{-1}^{1} |H_s(\xi)|^2\,d\xi \tag{B3}$$

where $u = \sin\theta$, $u_o = \sin\theta_o$, and $\xi = \sin\theta/\sin\theta_o$. The total energy radiated is

$$\int_{-\infty}^{\infty} |H_s(u)|^2\,du = \sin\theta_o \int_{-\infty}^{\infty} |H_s(\xi)|^2\,d\xi \tag{B4}$$

so that the ratio of the energy in the main beam to the total radiated energy is

$$R = \frac{\int_{-1}^{1} |H_s(\xi)|^2\,d\xi}{\int_{-\infty}^{\infty} |H_s(\xi)|^2\,d\xi}. \tag{B5}$$

In order to maximize Eq. (B5) it is convenient to expand the radiated field in terms of the angular prolate spheroidal functions $S_{on}(c,\xi) = S_{on}(c,\ \sin\theta/\sin\theta_o)$. That is, we write

$$H_s(\xi) = \sum_{n=0}^{\infty} a_n\,S_{on}(c,\,\xi). \tag{B6}$$

Now it can be shown that the prolate spheroidal functions have the following properties[8]

$$\int_{-\infty}^{\infty} S_{on}(c,\,\xi)\,S_{om}(c,\,\xi)\,d\xi = \delta_{nm}, \tag{B7}$$

8. Slepian, D., and Pollak, H. (1961) Prolate spheroidal wave functions, Fourier Analysis and Uncertainty I, Bell System Tech. J. 40:43-74.

$$\int_{-1}^{1} S_{on}(c, \xi)\, S_{om}(c, \xi)\, d\xi = \lambda_n \delta_{nm}, \tag{B8}$$

where δ_{nm} equals 0 if $n \neq m$ and equals 1 if $n = m$, and λ_n is given by

$$\lambda_n = \frac{2c}{\pi} \left[R_{on}(c, 1) \right]^2 \tag{B9}$$

where $R_{on}(c, \eta)$ is the radial prolate spheroidal function. The λ_n have the property that

$$\lambda_0 > \lambda_1 > \lambda_2 > \lambda_3 \cdots . \tag{B10}$$

One final useful property of S_{on} is

$$\left[2 i^n R_{on}(c, 1) \right] S_{on}(c, t) = \int_{-1}^{1} e^{icut} S_{on}(c, u)\, du . \tag{B11}$$

If we now use Eq. (B6) in (B5) and then employ the biorthogonality relationships in Eq. (B7) and Eq. (A8) we find that

$$R = \frac{\sum_{n=0}^{\infty} |a_n|^2 \lambda_n}{\sum_{n=0}^{\infty} |a_n|^2} . \tag{B12}$$

Finally, upon using Eq. (B10) it is clear that R is maximized when $a_n = 0$ for all n except n = 0. Therefore, the energy in the main beam is maximized when

$$H_s = S_{00}(c, \xi) = S_{00}\left(c, \frac{\sin\theta}{\sin\theta_o}\right) . \tag{B13}$$

A table of $S_{00}(c, \xi)$ for c = 5 and c = 6 is given in Table B1.

Table B1. Values of $S_{00}(c, \xi)$

ξ	$\frac{S_{00}(5, \xi)}{S_{00}(5, 0)}$	ξ	$\frac{S_{00}(6, \xi)}{S_{00}(6, 0)}$
0	1	0	1
0.0874	0.9842	0.174	0.924
0.174	0.9383	0.342	0.7314
0.259	0.8673	0.500	0.5012
0.342	0.7776	0.643	0.3026
0.424	0.6773	0.766	0.1653
0.500	0.5742	0.866	0.0850
0.575	0.4748	0.9659	0.0362
0.645	0.3989	1.0	0.0205
0.709	0.3046	1.0583	0.00564
0.768	0.2380	1.117	-0.00299
0.866	0.1419	1.1667	-0.00653
0.9307	0.08609	1.25	-0.00694
0.9848	0.05845	1.3333	-0.00364
1.000	0.05024	1.42	0.000478
1.07	0.01927	1.50	0.00356
1.14	-0.001257	1.58	0.00477
1.20	-0.011665	1.666	0.00414
1.40	-0.013556	1.75	0.00220
1.60	0.003182	1.835	-0.000190
1.80	0.01099	1.92	-0.00225
1.90	0.009285	2.083	-0.00339
2.0	0.005035		
2.2	-0.004719		
2.3	-0.007472		
2.4	-0.007858		

We next need to find the aperture distribution which yields the optimum radiation pattern expressed by Eq. (B13). Upon returning to Eq. (B1) we see that (ignoring the phase term)

$$H_s(\sin\theta) = \int_{-1}^{1} G(t)\, e^{i\left(\frac{2kF}{a}\right) t \sin\theta}\, dt . \qquad (B14)$$

Now from Eq. (B11) we have that

$$\mu S_{00}\left(c, \frac{\sin\theta}{\sin\theta_o}\right) = \int_{-1}^{1} S_{00}(c, t) \exp\left(i\, ct \frac{\sin\theta}{\sin\theta_o}\right) dt \tag{B15}$$

where $\mu = 2\, R_{00}(c, 1)$. Upon comparing Eqs. (A14) and (A15) it is clear that if $c = (2kF/a) \sin\theta_o$ the required aperture distribution G(t) must be

$$G(t) = S_{00}(c, t) = S_{00}\left(\frac{2kF}{a} \sin\theta_o, t\right) \tag{B16}$$

and that when this illumination is present on the aperture the radiation pattern is

$$H_s(\sin\theta) = S_{00}\left(\frac{2kF}{a} \sin\theta_o, \frac{\sin\theta}{\sin\theta_o}\right). \tag{B17}$$

Upon combining Eqs. (B16) and (B12) we see that the feed horn illumination pattern required to yield the radiation pattern in Eq. (B17) is

$$F_v(\psi) = \sec\left(\frac{\psi}{2}\right) S_{00}\left(\frac{2kF}{a} \sin\theta_o, a \tan\frac{\psi}{2} + b_o\right). \tag{B18}$$

A plot of the radiation pattern given by Eq. (B17) for $\theta_o = 1.52°$ and $(2kF \sin\theta_o/a) = 5$ is given by Figure B1. This radiation pattern has 99.9361 percent of its energy in the range $-1.52° < \theta_o < 1.52°$. The radiation pattern for $\theta_o = 1.82°$ and $(2kF \sin\theta_o/a) = 6$ is shown in Figure B2. This pattern has 99.9903 percent of its energy in the range $-1.82° < \theta_o < 1.82°$. It is clear from Figure B2 that if we design the reflector so that $2kF \sin\theta_o/a = 6$ we can easily (assuming reflector tolerances can be met) achieve sidelobes which are 50 dB or more below the main beam, once we are beyond the second sidelobe. The problem now is to design a feed to give us a radiation pattern

$$F_v(\psi) = \sec\left(\frac{\psi}{2}\right) S_{00}\left(6, a \tan\frac{\psi}{2} + b_o\right). \tag{B19}$$

In order to study Eq. (B19) further let us make the transformation $\psi = \phi + \Delta$ where $\tan(\Delta/2) = -(b/a)$. Then after using the trigonometric identities for the tangent of a sum of two angles we can rewrite Eq. (B19) as (ignoring the constant $[1 + b_o^2/a^2]^{1/2}$)

$$F_v(\phi) = \frac{S_{00}\left[6, \dfrac{a(1 + \frac{b_o^2}{a^2}) \tan\left(\frac{\phi}{2}\right)}{1 + \frac{b_o}{a} \tan(\phi/2)}\right]}{\cos\left(\frac{\phi}{2}\right) + \frac{b_o}{a} \sin\left(\frac{\phi}{2}\right)}. \tag{B20}$$

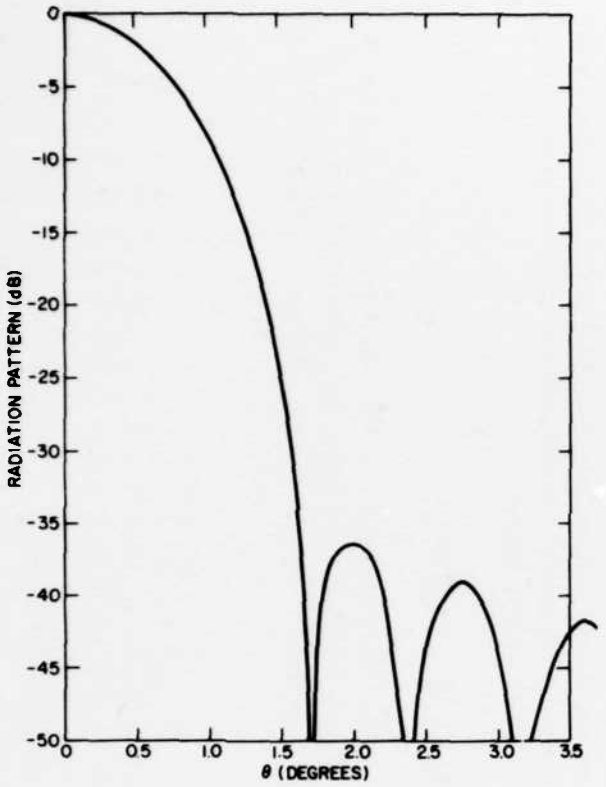

Figure B1. Radiation Pattern for $\theta_o = 1.52°$, $(2kF \sin \theta_o/a) = 5$. For this case $^{o}99.936$ percent of the energy is contained between $-1.52°$ and $+1.52°$

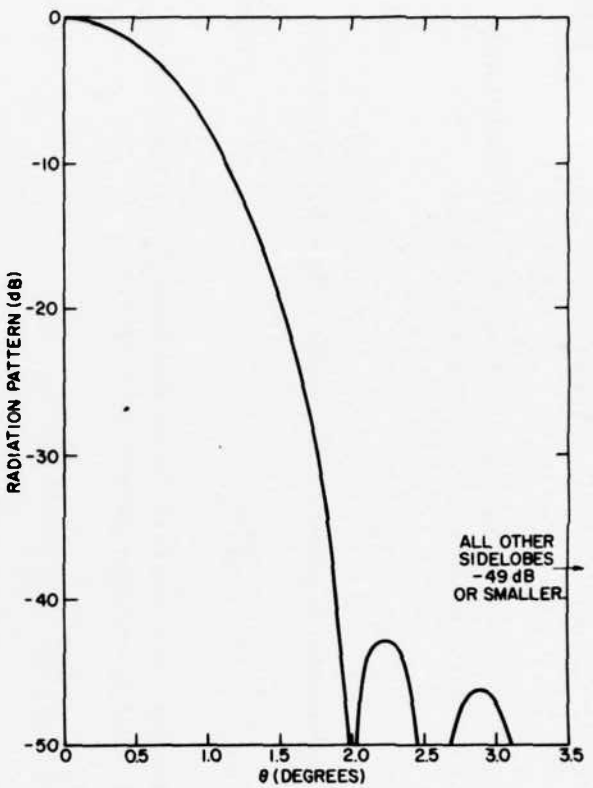

Figure B2. Radiation Pattern for $\theta_o = 1.82°$, $(2kF \sin \theta_o/a) = 6$. For this case $^{o}99.9903$ percent of the energy is contained between $-1.82°$ and $+1.82°$

We now assume that our reflector will be the portion of the parabolic cylinder shown in Figure B3. For this case it is evident that

$$-\frac{b_o}{a} = \frac{\tan\left(\frac{\psi_1}{2}\right) + \tan\left(\frac{\psi_o}{2}\right)}{2} < 1 \tag{B21}$$

because ψ_o and ψ_1 are both less than $\pi/2$. In addition it is also evident that $\phi/2 << 1$ so that

$$\tan\left(\frac{\phi}{2}\right) \simeq \frac{\phi}{2} \simeq \frac{\sin\phi}{2}. \tag{B22}$$

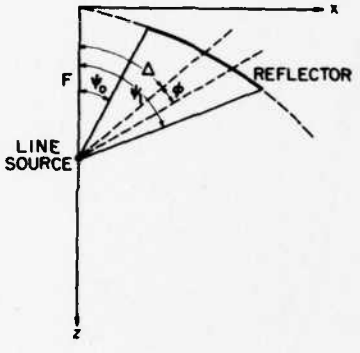

Figure B3. Geometry Used for Eq. (B21)

Therefore because $\phi/2 << 1$ we can rewrite Eq. (B10) as

$$F_v(\phi) \simeq S_{00}\left[6, \frac{a}{2}\left(1 + \frac{b_o^2}{a^2}\right)\sin\phi\right]. \tag{B23}$$

A comparison of this approximation with the exact result in Eq. (B19) for $\psi_o = 15°$ and $\psi_1 = 75°$ is shown in Figure B4.

We next desire to see if the approximate result in Eq. (B23) can be synthesized by a planar aperture lying in the focal plane of the reflector and oriented as shown in Figure B5. The electric field in the Fraunhofer zone due to a planar aperture of length 2L can be written as

$$E_R(\phi) = \int_{-1}^{1} T(y)\, e^{ikLy\sin\phi}\, dy \tag{B24}$$

where T(y) is the aperture distribution. If we equate Eq. (B24) to Eq. (B23) we get that T(y) must satisfy

$$S_{00}\left[6, \frac{a}{2}\left(1 + \frac{b_o^2}{a^2}\right)\sin\phi\right] = \int_{-1}^{1} T(y)\, e^{ikLy\sin\phi}\, dy. \tag{B25}$$

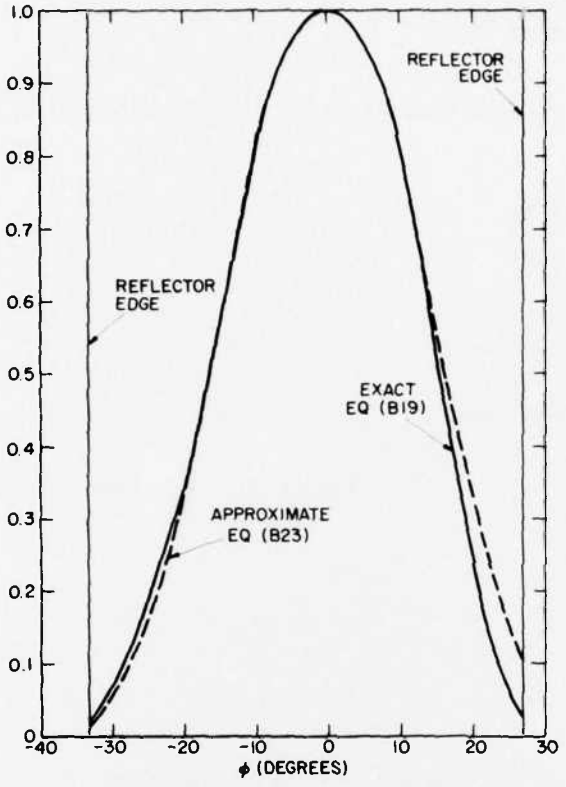

Figure B4. Comparison of the Approximation in Eq. (B23) With the Exact Result in Eq. (B19) for $\psi_o = 15°$, $\psi_1 = 75°$

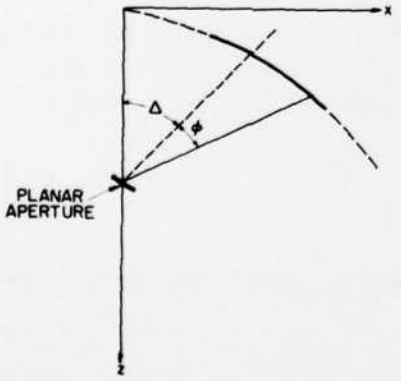

Figure B5. Geometry Used for Eqs. (B24) to (B28)

We can identify T(y) by using Eq. (B11). We readily find that (ignoring constants)

$$T(y) = S_{00}\left(6, \frac{y}{L}\right) \quad -L \le y \le L \tag{B26}$$

where

$$\frac{kL}{\frac{a}{2}\left(1 + \frac{b_o^2}{a^2}\right)} = 6 \tag{B27}$$

which means the aperture length 2L must be

$$2L = (3a/\pi)\left(1 + \frac{b_o^2}{a^2}\right)\lambda \ . \tag{B28}$$

In order to see what this means suppose we choose $\psi_o = 15°$ and $\psi_1 = 75°$; then $2L = 3.61\lambda$. This gives a feed radiation pattern $F_v(\phi) = S_{00}(6,\ 1.885 \sin \phi)$. For $\psi_o = 20°$ and $\psi_1 = 0°$ we get $2L = 4.35\lambda$ and this gives a feed radiation pattern $F_v(\psi) = S_{00}(6,\ 2.27 \sin \phi)$.

We have shown that the required feed aperture distribution is $S(6, \xi)$ for $-1 \le \xi \le 1$ where $\xi = y/L$. This function is an even monotonically decreasing function and can therefore be approximated (for $-1 \le \xi \le 1$) as

$$\frac{S_{00}(6,\ \xi)}{S_{00}(6,\ 0)} - \frac{S_{00}(6,\ 1)}{S_{00}(6,\ 0)} = \sum_{n=0}^{\infty} a_n \cos\left(\frac{2n+1}{2}\right)\pi\xi \ . \tag{B29}$$

The coefficients a_n can be determined by multiplying Eq. (B29) by $\cos\left(m + \frac{1}{2}\right)\pi\xi$ and integrating on ξ from -1 to 1. We find

$$a_n = \int_{-1}^{1} \frac{S_{00}(6,\ \xi)}{S_{00}(6,\ 0)} \cos\left[(2n+1)\frac{\pi\xi}{2}\right] d\xi - 2\frac{S_{00}(6,\ 1)}{S_{00}(6,\ 0)} \frac{\sin\left(n+\frac{1}{2}\right)\pi}{\left(n+\frac{1}{2}\right)\pi} \tag{B30}$$

If we note, because S_{00} is real and even, that

$$\int_{-1}^{1} S_{00}(6,\ \xi) \cos(\alpha\,\xi)\, d\xi = \int_{-1}^{1} S_{00}(6,\ \xi)\, e^{i\alpha\,\xi}\, d\xi$$

and then use Eq. (B11) we can evaluate the integral on Eq. (B30) to obtain

$$a_n = 2\, R_{00}(6,\ 1)\frac{S_{00}\left[6,\ \frac{(2n+1)\pi}{12}\right]}{S_{00}(6,\ 0)} - 2\frac{S_{00}(6,\ 1)}{S_{00}(6,\ 0)} \frac{\sin\left(n+\frac{1}{2}\right)\pi}{\left(n+\frac{1}{2}\right)\pi} \ . \tag{B31}$$

Values of a_n for the first few n are given in Table B2. From Table B2, we see that the required illumination function $S_{00}(6, \xi)/S_{00}(6, 0)$ can be approximately achieved by an illumination which has a constant term (over $-1 \le \xi \le 1$) equal to

$$\frac{S_{00}(6, 1)}{S_{00}(6, 0)} = 0.0205$$

plus the first two lowest order even waveguide modes, with the TE_{10} having an excitation of 0.8273 and the TE_{30} having the excitation 0.1569. That is, for $-1 \le \xi \le 1$

$$T(\xi) = \frac{S_{00}(6, \xi)}{S_{00}(6, 0)} = 0.0205 + 0.8273 \cos\left(\frac{\pi\xi}{L}\right) + 0.1569 \cos\left(\frac{3\pi\xi}{L}\right) \qquad \text{(B32)}$$

where $\xi = y/L$ and $2L$ is the length of the source. Therefore if we had a reflector subtended by the angle $15° \le \psi \le 75°$ (this requires $2L = 3.61\lambda$) we would need a feed distribution

$$T(y) = 0.0205 + 0.8273 \cos\left(\frac{\pi y}{2L}\right) + 0.1569 \cos\left(\frac{3\pi y}{2L}\right)$$

$$\text{for } -L \le y \le L \text{ and } 2L = 3.61\lambda. \qquad \text{(B33)}$$

Table B2. Values of a_n

n	a_n	Equivalent Waveguide Mode
0	0.8273	TE_{10} mode
1	0.1569	TE_{30} mode
2	-0.00987	TE_{50} mode
3	+0.003536	TE_{70} mode

METRIC SYSTEM

BASE UNITS:

Quantity	Unit	SI Symbol	Formula
length	metre	m	...
mass	kilogram	kg	...
time	second	s	...
electric current	ampere	A	...
thermodynamic temperature	kelvin	K	...
amount of substance	mole	mol	...
luminous intensity	candela	cd	...

SUPPLEMENTARY UNITS:

plane angle	radian	rad	...
solid angle	steradian	sr	...

DERIVED UNITS:

Acceleration	metre per second squared	...	m/s
activity (of a radioactive source)	disintegration per second	...	(disintegration)/s
angular acceleration	radian per second squared	...	rad/s
angular velocity	radian per second	...	rad/s
area	square metre	...	m
density	kilogram per cubic metre	...	kg/m
electric capacitance	farad	F	A·s/V
electrical conductance	siemens	S	A/V
electric field strength	volt per metre	...	V/m
electric inductance	henry	H	V·s/A
electric potential difference	volt	V	W/A
electric resistance	ohm		V/A
electromotive force	volt	V	W/A
energy	joule	J	N·m
entropy	joule per kelvin	...	J/k
force	newton	N	kg·m/s
frequency	hertz	Hz	(cycle)/s
illuminance	lux	lx	lm/m
luminance	candela per square metre	...	cd/m
luminous flux	lumen	lm	cd·sr
magnetic field strength	ampere per metre	...	A/m
magnetic flux	weber	Wb	V·s
magnetic flux density	tesla	T	Wb/m
magnetomotive force	ampere	A	...
power	watt	W	J/s
pressure	pascal	Pa	N/m
quantity of electricity	coulomb	C	A·s
quantity of heat	joule	J	N·m
radiant intensity	watt per steradian	...	W/sr
specific heat	joule per kilogram·kelvin	...	J/kg·K
stress	pascal	Pa	N/m
thermal conductivity	watt per metre·kelvin	...	W/m·K
velocity	metre per second	...	m/s
viscosity, dynamic	pascal·second	...	Pa·s
viscosity, kinematic	square metre per second	...	m/s
voltage	volt	V	W/A
volume	cubic metre	...	m
wavenumber	reciprocal metre	...	(wave)/m
work	joule	J	N·m

SI PREFIXES:

Multiplication Factors	Prefix	SI Symbol
1 000 000 000 000 = 10^{12}	tera	T
1 000 000 000 = 10^{9}	giga	G
1 000 000 = 10^{6}	mega	M
1 000 = 10^{3}	kilo	k
100 = 10^{2}	hecto*	h
10 = 10^{1}	deka*	da
0.1 = 10^{-1}	deci*	d
0.01 = 10^{-2}	centi*	c
0.001 = 10^{-3}	milli	m
0.000 001 = 10^{-6}	micro	μ
0.000 000 001 = 10^{-9}	nano	n
0.000 000 000 001 = 10^{-12}	pico	p
0.000 000 000 000 001 = 10^{-15}	femto	f
0.000 000 000 000 000 001 = 10^{-18}	atto	a

* To be avoided where possible


ATE
LMED
-7